Eur. Phys. J. B **13**, 695–699 (2000)

THE EUROPEAN PHYSICAL JOURNAL B

EDP Sciences

Antiferromagnetism and the node structure of the superconducting order parameter of UPd_2Al_3

M. Huth[a], M. Jourdan, and H. Adrian

Institute for Physics, Johannes Gutenberg-University Mainz, 55099 Mainz, Germany

Received 29 July 1999

Abstract. The node structure of the superconducting order parameter of the heavy-fermion system UPd_2Al_3 is analyzed within the weak-coupling theory. A pairing interaction induced by the exchange of antiferromagnetic spin excitations is assumed as suggested by recent inelastic neutron scattering experiments and tunneling spectroscopy. The multi-sheeted Fermi surface is taken into account. Based on a model susceptibility for the simple antiferromagnetic structure of UPd_2Al_3, line nodes result at the rim of the magnetic Brillouin zone.

PACS. 74.70.Tx Heavy-fermion superconductors – 74.20.Mn Nonconventional mechanisms (spin fluctuations, polarons and bipolarons, resonating valence bond model, anyon mechanism, marginal Fermi liquid, Luttinger liquid, etc.) – 74.50.+r Proximity effects, weak links, tunneling phenomena, and Josephson effects

1 Introduction

In the heavy-fermion system UPd_2Al_3 superconductivity below $T_c = 2$ K coexists with antiferromagnetic order setting in at $T_N = 14.5$ K [1]. The magnetic state of this hexagonal compound is formed by ferromagnetic easy planes of the U-moments stacked antiferromagnetically along the crystallographic c-axis [2].

Recent measurements of the characteristic energy losses for momentum transfers at and in the vicinity of the magnetic Bragg vector (001/2) showed two noticeable features: a strongly damped spin-wave excitation with an excitation energy of about 1.5 meV [3], and an energy loss peak in the superconducting state corresponding to the opening of the energy gap [4–6]. These neutron scattering results were corroborated by tunneling spectroscopy on cross-type $UPd_2Al_3/AlO_x/Pb$ tunnel junctions based on UPd_2Al_3 thin films [7,8]. A well developed energy gap along the crystallographic c-axis was observed. Furthermore, a modulation of the tunneling conductivity at an energy of about 1.2 meV was attributed to the coupling of the quasiparticle excitations to the antiferromagnetic spin wave. Strong-coupling effects in the tunneling density of states of conventional superconductors, like Pb and Hg, are caused by phonon modes that contribute the dominant part of the pairing interaction. In analogy, the strong-coupling effect observed in the UPd_2Al_3 tunneling spectra lends strong support to the assumption that the superconductivity in UPd_2Al_3 is caused by the exchange of antiferromagnetic spin excitations [8]. This is consistent with the observed pronounced Pauli-limiting in the upper critical field that indicates the formation of a singlet pairing state [9,10].

Assuming such a pairing interaction, quite general arguments can be given concerning the structure of the superconducting order parameter based on the known properties of UPd_2Al_3. Due to a pronounced magnetic anisotropy the spins tend to fluctuate in the basal planes [6]. It then follows that the pair partners cannot reside in the same plane due to a strong pair-breaking effect caused by the ferromagnetic spin alignment. The pairs might be formed by quasiparticles in neighbouring planes. This necessarily leads to a node in the spatial pair function for vanishing quasiparticle distance. Accordingly, the order parameter in k-space is anisotropic. We wish to substantiate these general arguments by analyzing the node structure of the superconducting order parameter on the multi-sheeted Fermi surface of UPd_2Al_3.

2 Derivation of the gap equation

Our analysis is based on a BCS pairing Hamiltonian in which the pairing interaction is governed by the momentum-dependent part of the dynamic spin susceptibility. This situation is similar to the case of conventional weak-coupling superconductors, where the zero-frequency limit of the phonon propagator plays the role of the potential for the phonon-mediated attraction between electrons [11]. Assuming a susceptibility that factorizes into a momentum- and an energy-dependent part the anisotropy of the order parameter in the weak-coupling and strong-coupling limit are identical. For the present analysis

[a] e-mail: huth@mail.uni-mainz.de

of the node structure it is then sufficient to limit the discussion to the weak-coupling limit. Strong-coupling effects in this compound are discussed elsewhere [12].

We use a Fermi gas model in which a strong zero-range repulsion I is acting between two quasiparticles with strong f-character having antiparallel spin. The resulting interaction Hamiltonian in the singlet channel reads [11]

$$\begin{aligned}\mathcal{H}_{\rm int} = -\frac{1}{4}\sum_{nn'}\sum_{\mathbf{k}\mathbf{k}'} J_{nn'}(\mathbf{k}-\mathbf{k}') \Big(&2a^+_{n\mathbf{k}\uparrow}a^+_{n-\mathbf{k}\downarrow}a_{n'-\mathbf{k}'\uparrow}a_{n'\mathbf{k}'\downarrow} \\ &+2a^+_{n\mathbf{k}\downarrow}a^+_{n-\mathbf{k}\uparrow}a_{n'-\mathbf{k}'\downarrow}a_{n'\mathbf{k}'\uparrow} \\ &-a^+_{n\mathbf{k}\uparrow}a^+_{n-\mathbf{k}\downarrow}a_{n'-\mathbf{k}'\downarrow}a_{n'\mathbf{k}'\uparrow} \\ &-a^+_{n\mathbf{k}\downarrow}a^+_{n-\mathbf{k}\uparrow}a_{n'-\mathbf{k}'\uparrow}a_{n'\mathbf{k}'\downarrow}\Big). \end{aligned} \quad (1)$$

The sum over the wave vectors $\mathbf{k}$, $\mathbf{k}'$ is limited to the respective bands n, n'. We express the coupling $J(\mathbf{q})$ in terms of the q-dependent susceptibility $\chi(\mathbf{q})$ within the random phase approximation

$$J_{nn'}(\mathbf{q}) = \frac{I}{2}\left(1 + I\chi_{nn'}(\mathbf{q})\right). \quad (2)$$

This crude approximation is justifiable if $\chi_{nn'}(\mathbf{q})$ is regarded as a phenomenological parameter, similar to the Landau parameters in Fermi liquid theory [11,13]. Its momentum dependence is, at least for selected regions in reciprocal space, accessible by experiment [14].

The pairing Hamiltonian

$$\mathcal{H} = \mathcal{H}_{\rm kin} + \mathcal{H}_{\rm int} = \sum_{n}\sum_{\mathbf{k}\sigma}\xi_{n\mathbf{k}}a^+_{n\mathbf{k}\sigma}a_{n\mathbf{k}\sigma} + \mathcal{H}_{\rm int} \quad (3)$$

can be diagonalized by a canonical transformation [15]. With the anomalous expectation values $b^{\sigma-\sigma}_{n\mathbf{k}}$ defined as

$$b^{\sigma-\sigma}_{n\mathbf{k}} = \langle a_{n-\mathbf{k}\sigma}a_{n\mathbf{k}-\sigma}\rangle, \quad (4)$$

and by introducing the new fermionic operators ($c_{n\mathbf{k}\alpha}$, $c_{n\mathbf{k}\beta}$)

$$\begin{aligned} a_{n\mathbf{k}\uparrow} &= u^*_{n\mathbf{k}}c_{n\mathbf{k}\alpha} + v_{n\mathbf{k}}c^+_{n\mathbf{k}\beta} \\ a^+_{n-\mathbf{k}\downarrow} &= -v^*_{n\mathbf{k}}c_{n\mathbf{k}\alpha} + u_{n\mathbf{k}}c^+_{n\mathbf{k}\beta}, \end{aligned} \quad (5)$$

the resulting mean-field Hamiltonian is diagonal provided that the following $T = 0$ self-consistency condition for the singlet order parameter $\Delta_{n\mathbf{k}} = 1/2 \times (\Delta^{\uparrow\downarrow}_{n\mathbf{k}} - \Delta^{\downarrow\uparrow}_{n\mathbf{k}})$ is fulfilled

$$\Delta_{n\mathbf{k}} = -\frac{1}{8}\sum_{n'}{\sum_{\mathbf{k}'}}' J_{nn'}(\mathbf{k}-\mathbf{k}')\frac{\Delta_{n'\mathbf{k}'}}{\sqrt{\xi^2_{n'\mathbf{k}'} + |\Delta_{n'\mathbf{k}}|^2}} \quad (6)$$

in which we used the following definition

$$\Delta^{\uparrow\downarrow}_{n\mathbf{k}} = -{\sum_{n'}}'\sum_{\mathbf{k}'} J_{nn'}(\mathbf{k}-\mathbf{k}')b^{\uparrow\downarrow}_{n'\mathbf{k}'}. \quad (7)$$

The prime on the momentum sum indicates the limitation to those $\mathbf{k}$-values within a small interaction shell such that $|\xi_{n'\mathbf{k}'}| < \epsilon_{\rm c}$. An important difference to the form of the self-consistency equation for electron-phonon coupling is manifest in the negative prefactor in equation (6). According to equation (2) $J_{nn'}$ is positive comprising a q-independent part that includes the local Coulomb repulsion and a q-dependent part governed by the susceptibility. As a result, the isotropic pairing interaction is repulsive. Solutions are possible if $J_{nn'}(\mathbf{q}) > 0$ peaks at some finite q-vector owing to the q-dependence of the susceptibility $\chi_{nn'}(\mathbf{q})$. The resulting pairing state can belong to the fully symmetric irreducible representation A_{1g} of the hexagonal point group D_{6h}, but must then exhibit line nodes in conjunction with sign changes of the order parameter on the Fermi surface. Alternatively, less symmetric one- or two-dimensional irreducible representations can be realized [16].

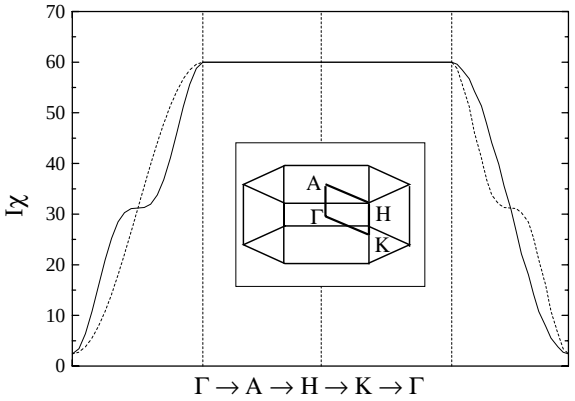

Fig. 1. q-dependent susceptibility according to equation (8) (dashed line) and (10) (solid line) along high symmetry directions of the Brillouin zone of the chemical unit cell (inset).

In the present case the spin-response function has to peak at the Brillouin zone boundary in z-direction (A-point) of the chemical unit cell due to the simple antiferromagnetic structure of UPd_2Al_3. As a consequence of the multi-sheet topology of the Fermi surface [17] intraband and interband transitions have to be considered. Lacking any detailed knowledge of the respective contributions to $\chi_{nn'}(\mathbf{q})$ we treat two limiting cases: $\chi_{nn'}(\mathbf{q}) = \chi(\mathbf{q})\delta_{nn'}$ or $\chi_{nn'}(\mathbf{q}) = \chi(\mathbf{q})$. On those parts of the Fermi surface which are most likely relevant to the pairing interaction, the q-dependence of the order parameter is essentially identical in these limiting cases, as will be shown below. Thus, even for a more realistic model, that properly includes inter- and intraband contributions, the node structure will not change significantly. Based on the simple antiferromagnetic structure of UPd_2Al_3 we use the following model form for $\chi(\mathbf{q})$

$$I\chi(\mathbf{q}) = I\chi_0\left[1 + b(1 - \cos(q_z c))\right] \quad (8)$$

which is shown in Figure 1 for various high-symmetry directions in the Brillouin zone of the chemical unit cell. $b = 10.5$ is chosen in correspondence with measurements of the static susceptibility and neutron-scattering results which give $\chi(q_z = \pi/c)/\chi(0) \simeq 20$ [18].

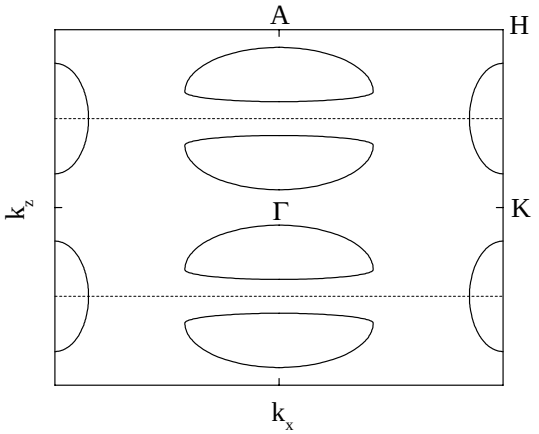

Fig. 2. Cross-sectional sketch of the Fermi surface of UPd_2Al_3 including only the sheets which were used in the calculations. The magnetic Brillouin zone is shown by the dashed lines. See text for details.

The self-consistency equation shall now be solved for the Fermi-surface of UPd_2Al_3. The Fermi surface consists of four sheets, three of which are electron-like and one hole-like [17]. This Fermi surface topology derived from band structure calculations is corroborated by de-Haas-van-Alphen measurements [19]. In the present case we have to estimate the relevance of the different sheets for the pairing interaction. From superconducting tunneling spectroscopy along the crystallographic c-axis we deduce that Fermi surface sheets having components along $\Gamma - A$ are important since an energy gap was observed in this direction [7,8]. This comprises the sheet which is commonly referred to as the "egg" part of the Fermi surface as shown in a cross-sectional view in Figure 2. Furthermore, the existence of line nodes of the superconducting order parameter is suggested by various experiments, such as nuclear magnetic resonance [20], thermal conductivity [21], and the angular dependence of the upper critical field measured on thin films [10]. As will be shown below, the q-dependent susceptibility induces the formation of line nodes on Fermi-surface sheets centered between the K- and H-point. We therefore include the electron-like Fermi surface sheet referred to as "cigar". Contributions from the remaining two sheets are unlikely. Their inherent two-dimensional topology should be reflected in a strongly anisotropic contribution to the superconducting properties which have not been observed in UPd_2Al_3. We therefore exclude these Fermi surface sheets from our analysis. The possibility of the existence of different electron substates of $5f$ character, only one of which involving the heavy quasiparticles, was already discussed in the analysis of pressure-dependent specific heat measurements [22] and muon spin rotation experiments [23]. Clear differences in the degree of $5f$ orbital character on the different Fermi surface sheets were also deduced from the band structure calculations [17]. In this context we refer to analogous considerations which were drawn from the dispersion of the spin-excitations close to the antiferromagnetic Bragg point [14]. Nevertheless, the assumption of the Fermi surface having parts that do not contribute to the condensate poses some problems. Additional low-energy excitations result which should be detectable in specific heat and various other measurements. This issue might be resolved in conjunction with the opening of an excitation gap in the antiferromagnetic state, as was deduced by the low-temperature behaviour of the electrical resistivity [24] and shown directly by inelastic neutron scattering experiments [4–6].

With the onset of antiferromagnetic order the symmetry is reduced to orthorhombic with the moments pointing along the x-axis. Since the deviations from hexagonal symmetry are small [17], they are ignored in our analysis. We furthermore simplify the Fermi surface to uniaxial anisotropy, *i.e.* the Fermi surface used for our calculation is obtained by rotating the cross-sectional sketch shown in Figure 2 around the $\Gamma - A$ axis. Due to the ellipsoidal topology of the "eggs" and "cigars" we use an effective mass model for the quasiparticle dispersion $\xi_{\mathbf{q}}$. This results in the following form of equation (6)

$$\Delta_{n\mathbf{k}} = -\frac{\mathrm{Vol}}{(2\pi)^2}\frac{m_0c^2}{(\hbar c)^2}\sum_{n'}\sum_{\mathbf{k}'\in S_{F'}}\frac{Im^*_{n'}/m_0}{16} \times \int_0^{\pi} \mathrm{d}\theta_{k'}|\mathbf{k}'|\sin\theta_{k'}\,(1+I\chi(\mathbf{k}-\mathbf{k}'))\,\Delta_{n'\mathbf{k}'} \times \ln\left(\frac{\epsilon_\mathrm{c}+\sqrt{\epsilon_\mathrm{c}^2+|\Delta_{n'\mathbf{k}'}|^2}}{\epsilon_\mathrm{c}+\sqrt{\epsilon_\mathrm{c}^2-|\Delta_{n'\mathbf{k}'}|^2}}\right). \quad (9)$$

$\theta_{k'}$ is the polar angle on the respective Fermi surface sheets.

This equation is solved by numerical integration and iteration until self-consistency is obtained. The parameter values are chosen as follows: effective band masses $m^*_{n'}/m_0 = 1$, $I\chi_0 = 2.4$ and $I = 230$ meV from the band structure calculations [17], and the cutoff energy $\epsilon_\mathrm{c} = 4$ meV. As a starting point for the iteration the initial form of the order parameter is chosen to be symmetric with respect to the Γ point. The gap size on the "egg" and "cigar" part of the Fermi surface is initially set to 0.3 meV in accordance with the gap size from our tunneling experiments. The result based on the model susceptibility of equation (8) are shown in Figure 3a including interband transitions. We obtain a node-less but anisotropic order parameter on the "egg" parts of the Fermi surface and line nodes on the "cigars". The gap sizes, as summarized in Table 1, have the right order of magnitude when compared to the experimental value measured for the "egg" sheets [8]. Nevertheless, the obtained anisotropy on the "eggs" is too pronounced. The tunneling experiments show a single gap-like structure in the c-axis direction. Since in the tunneling experiments the broken translational symmetry across the tunneling barrier leads to an averaging of all the gap sizes in c-direction, the resulting tunneling density of states according to our calculation would result in a double-gap feature. This is shown in Figure 4a (dashed line). This result is a direct consequence of the simple form we chose for the q-dependent susceptibility. As can be seen for the "egg" topology, Fermi

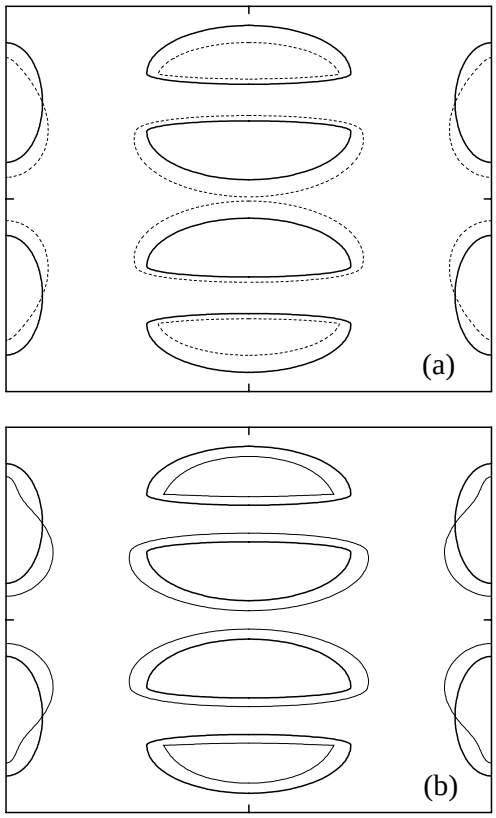

Fig. 3. The order parameter on the different Fermi surface sheets according to the q-dependent susceptibilities in (a) equation (8) and (b) equation (10). The Fermi surface sheets are shown in thick lines. The size of the order parameter is parameterized by the distance to the respective Fermi-surface sheets. The sign of the order parameter is positive if drawn on the outside of the Fermi surface and negative if drawn on the inside.

Table 1. Calculated order parameter excluding interband transitions (#1, #2) and including interband transitions (#3, #4) using the q-dependent susceptibilities as indicated. See text for details.

#	Sheet	$\chi(\mathbf{q})$	$\Delta(\theta=0)$ (meV)	$\Delta(\theta=\pi)$ (meV)	$\frac{\Delta(\pi)}{\Delta(0)}$
1	"eggs"	χ Eq. (8)	0.08	0.25	3.1
2	"eggs"	χ Eq. (10)	0.13	0.16	1.2
3	"eggs"	χ Eq. (8)	0.17	0.56	3.3
	"cigars"		−0.49	0.49	−1.0
4	"eggs"	χ Eq. (10)	0.31	0.36	1.2
	"cigars"		−0.50	0.50	−1.0

surface nesting effects might be important and add additional structure to the q-dependence. To illustrate this effect we modify the susceptibility to

$$I\chi(\mathbf{q}) = I\chi_0\left[1 + b(4/3 - \cos(q_z c) - 1/3\cos(3q_z c))\right] \tag{10}$$

with $b = 8.0$ which now comprises the first two elements of the Fourier series for a staggered moment in c-direction (see Fig. 1). The resulting order parameter is shown in

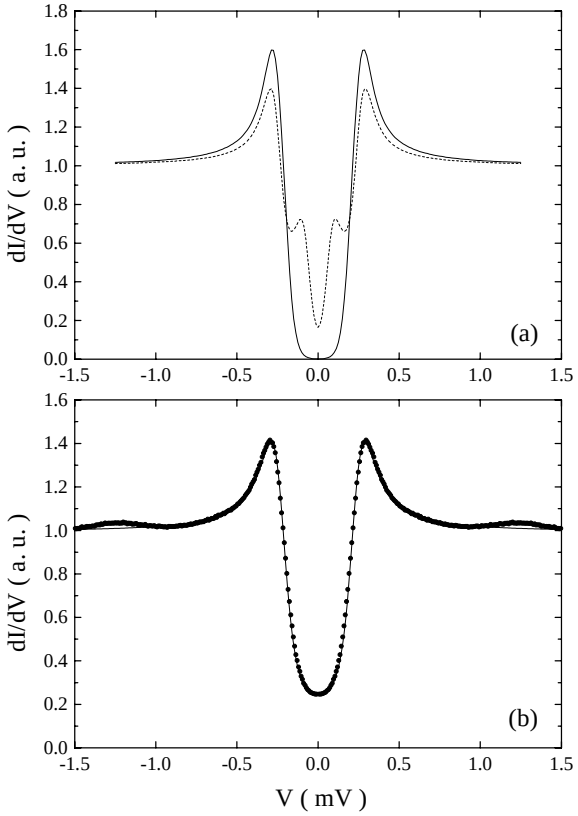

Fig. 4. (a) Calculated differential conductivities at $T = 0.3$ K for two different gap anisotropies according to the q-dependent susceptibility given in equation (8) (dashed line) and equation (10) (solid line). (b) Measured differential conductivity at $T = 0.3$ K in an applied magnetic field of 0.3 T. The solid line corresponds to a fit of the data using the Dynes formula with a gap size of $\Delta = 235$ μeV, a broadening parameter of 35 μeV, and a leakage conductivity of 0.1 a.u. [8].

Figure 3b. Figure 4a (solid line) shows the respective differential conductivity. The gap anisotropy along the $\Gamma - A$ direction on the "eggs" is now reduced to about 20 percent which could account for part of the observed broadening in the tunneling experiments shown in Figure 4b.

Any further improvements would have to rely on a better knowledge of the q-dependent susceptibility. Also, the energy-dependence of the order parameter has been ignored. By including strong-coupling effects the measured conductivity modulation at about 1.2 meV can be related to the magnon excitation observed in the neutron-scattering experiments. First results based on the Eliashberg theory are presented elsewhere [12].

3 Conclusion

We conclude by discussing the node structure proposed here with respect to the experimental information available so far. Inelastic neutron scattering experiments and tunneling spectroscopy have shown that an energy gap in c-direction exists. The visibility of the energy gap in the neutron scattering experiments at the magnetic Bragg

point implies that the pair function is periodically changing its sign in c-direction analogous to the magnetic order parameter. In this context we specifically refer to [14]. Further experimental results point towards line nodes in the order parameter. Nodes and sign changes of the superconducting order parameter cannot be justified on the basis of a pure electron-phonon coupling mechanism. On the other hand, within our model assumptions of antiferromagnetic spin-excitation coupling they are mandatory based on the given Fermi surface. Furthermore, a strong-coupling feature observed in the tunneling experiments gives evidence for a spin-excitation pairing interaction in analogy to the reasoning used in conventional superconductors. Consequently, antiferromagnetic pair coupling is very likely to be the reason for superconductivity in UPd_2Al_3.

We consider the following issues to be highly interesting for further investigations. On the theoretical side, T_c calculations based on the Eliashberg strong-coupling theory would be desirable. These would have to show that a T_c of about 2 K is possible for a magnetic pairing mechanism in UPd_2Al_3. It would also have to be shown that the order parameter transforming according to the higher order basis functions of the A_{1g}-representation results indeed in the largest T_c. On the experimental side, investigations of the gap anisotropy are needed. So far, an analysis of the angular dependence of the upper critical field was performed for a simplified one-sheet ellipsoidal Fermi surface [10]. This has to be redone based on the now known Fermi surface in order to separate Fermi-surface induced anisotropies in H_{c2} from those anisotropies which might be due to nodes in the order parameter. One of the most direct probes for the gap anisotropy is given by tunneling spectroscopy along various crystallographic directions. Additionally, pair-tunneling is sensitive to the phase changes of the superconducting order parameter. We believe that thin film investigations can make further important contributions to this field.

During the preparation of this manuscript M. H. enjoyed stimulating and helpful discussions with N. Bernhoeft, A. Goltsev, F. Anders, and L. Sandratskii. This work was supported by the Deutsche Forschungsgemeinschaft through SFB 252.

References

1. C. Geibel, C. Schank, S. Thies, H. Kitazawa, C.D. Bredl, A. Böhm, M. Rau, A. Grauel, R. Caspary, R. Helfrich, U. Ahlheim, G. Weber, F. Steglich, Z. Phys. B **84**, 1 (1991).
2. A. Krimmel, P. Fischer, B. Roessli, H. Maletta, C. Geibel, C. Schank, A. Grauel, A. Loidl, F. Steglich, Z. Phys. B **86**, 161 (1992).
3. T. Petersen, T.E. Mason, G. Aeppli, A.P. Ramirez, E. Bucher, R.N. Kleinman, Physica B **199-200**, 151 (1994); N. Sato, N. Aso, G.H. Lander, B. Roessli, T. Komatsubara, Y. Endoh, J. Phys. Soc. Jpn. **66**, 1884 (1997); N. Metoki, Y. Haga, Y. Koike, N. Aso, Y. Onuki, J. Phys. Soc. Jpn. **66**, 2560 (1997).
4. N. Metoki, Y. Haga, Y. Koike, Y. Onuki, Phys. Rev. Lett. **80**, 5417 (1998).
5. N. Bernhoeft, B. Roessli, N. Sato, N. Aso, A. Hiess, G.H. Lander, Y. Endoh, T. Komatsubara, in *Itinerant Electron Magnetism: Fluctuation Effects*, edited by D. Wagner, W. Brauneck, A. Solontsov (Kluwer, 1998); N. Bernhoeft, B. Roessli, N. Sato, N. Aso, A. Hiess, G.H. Lander, Y. Endoh, T. Komatsubara, Physica B **259-261**, 614 (1999).
6. N. Bernhoeft, B. Roessli, N. Sato, N. Aso, A. Hiess, G.H. Lander, Y. Endoh, T. Komatsubara, Phys. Rev. Lett. **81**, 4244 (1998).
7. M. Jourdan, M. Huth, H. Adrian, Physica B **259-261**, 621 (1999).
8. M. Jourdan, M. Huth, H. Adrian, Nature **398**, 47 (1999).
9. K. Gloos, R. Modler, H. Schimanski, C.D. Bredl, C. Geibel, F. Steglich, A.I. Buzdin, N. Sato, T. Komatsubara, Phys. Rev. Lett. **70**, 501 (1993).
10. J. Hessert, M. Huth, M. Jourdan, H. Adrian, C.T. Rieck, K. Scharnberg, Physica B **230-232**, 373 (1997).
11. S. Nakajima, Progr. Theor. Phys. **50**, 1101 (1973).
12. M. Huth, M. Jourdan in *Festkörperprobleme/Advances in Solid State Physics 39*, edited by B. Kramer (Vieweg, Braunschweig/Wiesbaden, 1999), p. 351; M. Huth, M. Jourdan, H. Adrian, conference on *Strongly Correlated Electron Systems (SCES'99)* (Nagano, Japan, 1999), accepted for publication in Physica B.
13. K. Miyake, S. Schmitt-Rink, C.M. Varma, Phys. Rev. B **34**, 6554 (1986).
14. N. Bernhoeft, Eur. Phys. J. B **13**, 685 (2000).
15. See *e.g.* M. Tinkham, *Introduction to Superconductivity* (McGraw-Hill, New York, 1975).
16. S. Yip, A. Garg, Phys. Rev. B **48**, 3304 (1993).
17. L.M. Sandratskii, J. Kübler, P. Zahn, I. Mertig, Phys. Rev. B **50**, 15834 (1994); K. Knöpfle, A. Mavromaras, L.M. Sandratskii, J. Kübler, J. Phys. Cond. Matter **8**, 901 (1996).
18. N. Bernhoeft (private communication).
19. Y. Inada, H. Aono, A. Ishiguro, J. Kimura, N. Sato, A. Sawada, T. Komatsubara, Physica B **119-200**, 119 (1994).
20. M. Kyogaku, Y. Kitaoka, K. Asayama, C. Geibel, C. Schank, F. Steglich, J. Phys. Soc. Jpn. **62**, 4016 (1993); K. Matsuda, Y. Kohori, T. Kohara, Phys. Rev. B **55**, 15223 (1997); K. Matsuda, Y. Kohori, T. Kohara, Physica B **259-261**, 640 (1999).
21. M. Hiroi, M. Sera, N. Kobayashi, Y. Haga, E. Yamamoto, Y. Onuki, J. Phys. Soc. Jpn. **66**, 1595 (1997).
22. R. Caspary, P. Hellmann, M. Keller, G. Sparn, C. Wassiliew, R. Köhler, C. Geibel, C. Schank, F. Steglich, N.E. Phillips, Phys. Rev. Lett. **71**, 2146 (1993).
23. R. Feyerherm, A. Amato, F.N. Gygax, A. Schenck, C. Geibel, F. Steglich, N. Sato, T. Komatsubara, Phys. Rev. Lett. **73**, 1849 (1993).
24. M. Huth, A. Kaldowski, J. Hessert, Th. Steinborn, H. Adrian, Solid State Commun. **87**, 1133 (1993).